Journal of Paleolimnology **31:** 235–252, 2004.
© 2004 *Kluwer Academic Publishers. Printed in the Netherlands.*

Record of Late Pleistocene glaciation and deglaciation in the southern Cascade Range. II. Flux of glacial flour in a sediment core from Upper Klamath Lake, Oregon★

Joseph G. Rosenbaum* and Richard L. Reynolds
*US Geological Survey, Box 25046, MS 980, Federal Center, Denver, CO 80225, USA; *Author for correspondence (e-mail: jrosenbaum@usgs.gov)*

Received 1 May 2002; accepted in revised form 2 July 2003

Key words: Glacial flour, Lacustrine sediment, Late Pleistocene, Paleoclimate, Sediment magnetism

Abstract

During the late Wisconsin, glacial flour from alpine glaciers along the east side of the Cascade Range in southern Oregon was deposited in Upper Klamath Lake. Quantitative interpretation of magnetic properties and grain-size data of cored sediments from Caledonia Marsh on the west side of the lake provides a continuous record of the flux of glacial flour spanning the last ≈37 000 calendar years. For modeling purposes, the lake sediments from the 13-m core were divided into three sedimentary components defined from magnetic, geochemical, petrographic, and grain-size data. The components are (1) strongly magnetic, glacial flour made up of extremely fine-grained, fresh volcanic rock particles, (2) less magnetic lithic material made up of coarser, weathered volcanic detritus, and (3) non-magnetic biogenic material (largely biogenic silica). Quantitative interpretation is possible because there has been no significant postdepositional destruction or formation of magnetic minerals, nor alteration affecting grain-size distributions. Major steps involved in the interpretation include: (1) computation of biogenic and lithic components; (2) determination of magnetic properties and grain-size distributions of the non-glacial and glacial flour end-members; (3) computation of the contents of weathered and glacial flour components for each sample; (4) development of an age model based on the mass accumulation of the non-glacial lithic component; and (5) use of the age model and glacial flour contents to compute the flux of glacial flour. Comparison of the glacial flour record from Upper Klamath Lake to mapped glacial features suggests a nearly linear relation between flux of glacial flour and the extent of nearby glaciers. At ≈22 ka, following an extended period during which glaciers of limited size waxed and waned, late Wisconsin (Waban) glaciers began to grow, reaching their maximum extent at ≈19 ka. Glaciers remained near their maximum extent for ≈1000 years. During this period, lake sediments were made up of ≈80% glacial flour. The content of glacial flour decreased as the glaciers receded, and reached undetectable levels by 14 ka.

Introduction

Two methods have been used to derive the history of alpine glaciation. The more common method involves mapping and stratigraphic interpretation of glacial deposits. The other method interprets variations in glacial extent from sediments in lakes that have received fluvial input of glacially derived material

★This is the seventh in a series of eight papers published in this special issue, resulting from paleoenvironmental studies in the Upper Klamath Lake Basin. These studies were conducted by the U.S. Geological Survey and its collaborators as part of a paleoclimate research effort called the Correlation of Marine and Terrestrial Records Project. Steven M. Colman served as guest editor of this special issue.

(Leonard 1985; Karlén and Matthews 1992). Both methods have advantages and disadvantages.

As an advantage, mapping is the only way to determine the actual extent of glaciers. Glacial extents combined with hypsometric analysis allow estimates of past equilibrium line altitudes. As a disadvantage, glaciers erode older deposits so that the glacial record is poorly preserved. Stratigraphic correlations, which commonly rely upon weathering indexes, are difficult to extend to areas with differing climates or rock types. Absolute age control is difficult even for deposits within the range of ^{14}C dating although cosmogenic nuclide methods have recently yielded glacial chronologies (e.g., Phillips et al. 1996). Continuous, well-dated records that provide information about the timing and duration of advances, still stands, and retreats cannot be obtained.

On the other hand, sediment records from proglacial lakes potentially provide continuous records of glaciation, recording advances and retreats as well as maximum extents. Continuous deposition leads to strong stratigraphic relations, and, for late Wisconsin and younger periods, ^{14}C ages may be obtained from organic material incorporated in the lake sediment. Sedimentary records, however, do not provide direct information about the absolute size and distribution of glaciers. Although short-term fluctuations in glacial flour output may reflect subglacial storage and subsequent flushing by high runoff events, Leonard (1997) argues persuasively that longer-term output of glacial flour (averaged over tens to hundreds of years) largely reflects glacial extent. Nevertheless, there is considerable uncertainty about the timing and controls of glacial sediment discharge (Hicks et al. 1990; Karlén and Matthews 1992; Harbor and Warburton 1993; Hallet et al. 1996; Leonard 1997).

Sediments in a 13-m long core from Caledonia Marsh at Upper Klamath Lake, Oregon, span about the last 40 000 years (Colman et al. 2004 – this issue) and provide a record for late Wisconsin glaciation of the southern Cascade Range. Reynolds et al. (2004 – this issue) presented magnetic properties, petrographic observations, geochemical and grain size data from the core. They demonstrated that, throughout much of marine oxygen isotope stages (OIS) 2 and 3 (37–14 ka), variations in bulk sediment grain size and magnetic properties were produced largely by variations in the mixture of fine-grained, highly magnetic glacial flour, consisting of fresh volcanic rock fragments, and somewhat coarser, less magnetic weathered lithic material. Here we extend interpretation of these data to derive estimates of the flux of glacial flour at the core locality. Variation in the flux of glacial flour constitutes a continuous, high-resolution ^{14}C-dated record of late Wisconsin glaciation of mountains to the west and northwest of the lake. The lake record can be compared to the history of glaciation in the catchment determined from mapping and stratigraphic studies (Carver 1973). This comparison clarifies relations between glacial extents and glacial flour discharge. The timing and amplitude of southern Cascade glaciation can also be compared to the record of global ice volume and to other regional glacial records in western North America. For the southern Cascades, these comparisons illustrate that; (1) maximum glacial extent ($\approx$19–18 ka) occurred after the Last Glacial Maximum
($\approx$21 ka), (2) deglaciation occurred at about the same time as in other parts of the Cascades as well as the Sierra Nevada and Rocky Mountains, and (3) glacial advances may be correlative with each of four Tioga advances in the eastern Sierra Nevada.

Rationale

This study differs in a number of important aspects from other studies that have used lake sediments to interpret glacial history and from studies that have used magnetic properties to reconstruct environmental change.

Studies of alpine glacial history from lake sediments have used either cores from proglacial lakes that received material from a single glacier, or from lakes receiving input from larger, more complex drainage basins. Studies of proglacial lakes have used various techniques to estimate the proportions of organic and lithic material. Qualitative interpretations have been based on the assumptions that lithic content increases as glacially derived sediment increases, and that the amount of glacial sediment reflects the extent of glaciation (Karlén 1976, 1981; Karlén and Matthews 1992; Leonard 1985, 1986, 1997). Owens Lake (California) is an example of a lake that received sediment, including glacial flour, from a large

complex catchment (Smith and Bischoff 1997). Non-biological environmental proxies at Owens Lake, which include geochemical parameters (Bischoff et al. 1997), bulk sediment grain size (Menking 1997), and magnetic susceptibility (Benson et al. 1996), reflect changes in lake level and concomitant changes in water chemistry and authigenesis as well as changes in detrital input (Smith et al. 1997; Reynolds et al. 1998). At Owens Lake, mineralogy of the clay-size fraction provides the most direct measure of glacial flour (Menking 1997; Bischoff and Cummins 2001).

In this study we use an innovative interpretation of geochemical, bulk sediment grain size, and magnetic property data to quantify the flux of glacial flour at the coring site in Upper Klamath Lake. Upper Klamath Lake, like Owens Lake, received sediment from a large catchment and acquired glacial flour from a number of nearby valley glaciers (Reynolds et al. 2004 – this issue; Carver 1973). Interpretation of the detrital record for Upper Klamath Lake, however, is much simpler than for Owens Lake because, for the entire time interval represented by the Caledonia Marsh core, Upper Klamath Lake was fresh, over flowing, and changed little (if any) in size (Bradbury et al. 2004 – this issue).

Magnetic properties that provide quantitative measures of the amount and type of magnetic minerals are valuable for paleoenvironmental studies, because these properties commonly vary with changing conditions indicated by biologic and isotopic proxies (Verosub and Roberts 1995; Reynolds and King 1995). Although measurements of magnetic properties are extremely accurate, most interpretations of magnetic data are qualitative because, in most lacustrine settings, there is insufficient information to fully unravel the combined effects of various physical and chemical processes. For example, magnetic properties of sediments may be affected by: (1) changes in provenance of detrital material, (2) changes in weathering and sediment transport, (3) dilution by biogenic (e.g., organic compounds and biogenic silica) and authigenic material (e.g., carbonate minerals), and (4) authigenic destruction or formation of magnetic phases. One method for making a quantitative interpretation is to use an empirical relation between magnetic properties and some environmental parameter to establish the magnetic measurements as proxies (e.g., Maher et al. 1994a,b; Liu et al. 1995). Another approach requires analyzing each of the processes that affect magnetic properties in order to construct a quantitative model. This second approach, used here, is only feasible in relative simple depositional systems such as that represented by sediments in the Caledonia Marsh core. In these sediments, magnetic properties vary largely as a function of changing proportions of glacial flour and more highly weathered lithic material as well as dilution by biogenic material (Reynolds et al. 2004 – this issue; Rosenbaum and Reynolds 2004 – this issue). Importantly, there was no significant post-depositional formation or destruction of magnetic minerals. Additionally, sedimentological complexities associated with lake level change and deltaic environments have been avoided because the lake overflowed continuously (Bradbury et al. this issue), and because the coring site is remote from major sediment sources (Reynolds et al. 2004 – this issue). Finally, no glaciated drainages enter the lake near the core site so that only fine-grained glacial silt, which could remain in suspension for an extended period, was deposited at this location and this material represents the combined input from several valley glaciers.

Overview of the models

Two models were developed to determine the flux of glacial flour through time by calculating the mass of glacial flour and time increment for each sample interval (Figure 1). One model is based primarily on magnetic properties (model 1) and the other is based primarily on sediment grain-size data (model 2). In both models the sediment is comprised of three components, a biogenic component and two lithic components. The content of each component is determined on a sample-by-sample basis. The biogenic component, which is made up of organic material and biogenic silica, is determined from geochemical measurements and is identical in both models. Although the biogenic material is diamagnetic (i.e., it has a small negative magnetic susceptibility), it is considered nonmagnetic for modeling purposes. The two lithic components, non-glacial detritus and glacial flour, are mineralogically similar (being derived from similar volcanic rocks) but have different physical

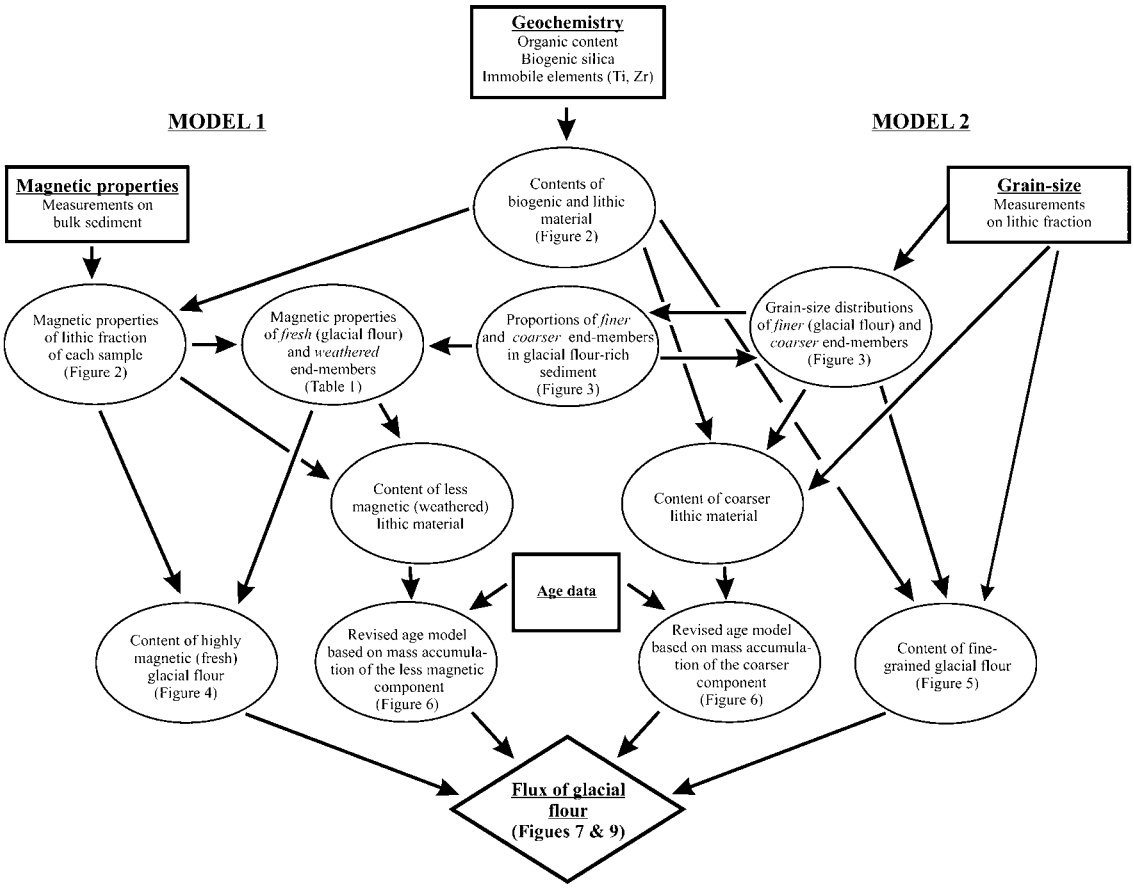

Figure 1. Schematic diagram showing steps in determining the flux of glacial flour. Data sets are indicated by rectangles and intermediate results in ovals.

properties. The glacial flour is finer grained and more highly magnetic than the non-glacial material (Reynolds et al. 2004 – this issue). With the exception of tephra in a few samples, all detrital particles in the sediments are less than 325.5 μm. Therefore, grain-size distributions used in the analysis comprise the weight percent of material in each of 38 size classes spanning 0.53–325.5 μm. Smaller clay-sized material was ignored because it may have been affected by treatment to remove biogenic silica. Two magnetic parameters, magnetic susceptibility (MS) and anhysteretic remanent magnetization (ARM), were used in model 1. Both parameters are largely a measure of the quantity of titanomagnetite, but ARM is more sensitive to small magnetic grain sizes (single and pseudo-single domain grains), whereas, MS is more sensitive to larger (multi-domain) grain sizes (King et al. 1982; Dunlop and Özdemir 1997). The two parameters should yield nearly identical results if the model is valid and the lithic end-members have been correctly characterized.

A major assumption for both models is that the sediment contains only the three components described above. The other major assumption for model 1 is that the magnetic properties of the lithic end-members can be accurately defined and remain constant throughout the length of the core. Similarly, a major assumption for model 2 is that the grain-size distributions of the end-members can be defined and remain constant. These assumptions are reasonable in light of thorough analyses that did not reveal any post-depositional production of minerals or destruction of detrital minerals (Reynolds et al. 2004 – this issue). With these assumptions, the fraction of each lithic end-member

in each sample can be calculated from magnetic properties and independently from grain-size data. In practice, the models are not totally independent because, as described below, grain-size data were used in defining the magnetic properties of the glacial flour end-member. Nevertheless, comparison of the results of the two models lends credence to the interpretations.

The time span represented by a given sedimentary interval is determined from the slope of a depth *versus* age curve. Abrupt changes in slope, as may exist for a curve comprised of linear segments, produce abrupt changes in calculated flux that are artifacts of the depth/age model. Because changes in the flux of the non-glacial lithic component were of smaller magnitude and less abrupt than changes in the flux of glacial flour, a model based on the mass accumulation of the non-glacial component was used in place of the original age model for the core (Colman et al. 2004 – this issue). For each sample, fluxes of glacial flour were then calculated from the results of models 1 and 2 and the revised age model.

Biogenic component

Organic matter and diatoms (opaline silica) make up the biogenic component of the sediment. Significant amounts of organic matter occur only in the mid- to late-Holocene sediments, but diatoms are present in significant quantities throughout the core (Bradbury et al. 2004 – this issue). Because measurements of opaline silica are relatively time consuming and costly, the biogenic component was computed from values of Ti and Zr.

Ti and Zr are contained in the lithic components but not in the biogenic component; therefore, the quantities of these chemically immobile elements vary inversely with the biogenic component. Ti and Zr were measured in 70 of the 225 samples used for magnetic property measurements (Reynolds et al. 2004 – this issue). The ratio, Zr/Ti, which varies with rock composition (Winchester and Floyd 1977), shows little variation with depth (Reynolds et al. 2004 – this issue) so that variations due to changes in provenance can be discounted.

In order to calibrate Ti and Zr as proxies for the biogenic component, these elements were compared to the biogenic content for 11 samples (Figure 2). The biogenic component is the sum of biogenic silica and organic matter (Bradbury et al. 2004 – this issue). These 11 samples yielded average values for the lithic fraction of 0.593% for Ti and 177 ppm for Zr. Biogenic fractions calculated using these values are nearly identical (Figure 2). Biogenic-free values of MS and ARM were calculated using the Ti-based estimates. (Note: All samples below 12.25 m lack geochemical data and were assigned the calculated biogenic content of the sample at that depth. Above 12.25 m, values of biogenic content were interpolated for samples lacking geochemical data.)

Properties of the lithic end-members

Before the fractions of the two lithic end-members in each sample can be calculated, the end-members must be characterized in terms of magnetic properties and grain-size. Representative grain-size distributions and magnetic properties of the non-glacial end-member are readily determined from post-glacial sediment, which contains no glacial flour. Estimation of physical properties for glacial flour, however, is more complex because all samples contain some non-glacial material. Average magnetic properties of volcanic rocks in the catchment cannot be used to characterize the glacial flour because of the effects of hydrodynamic sorting (Rosenbaum and Reynolds 2004 – this issue; Nesbitt and Young 1996). Therefore, the average content of nonglacial material in glacial flour-rich sediment was estimated by comparison of grain-size distributions as described below. This estimate was then used to calculate the grain-size distribution and magnetic properties of glacial flour.

Average properties for the non-glacial end-member were calculated from five samples in the interval 4.11–4.87 m (Figure 3A and Table 1). Sediments in this interval were chosen to represent the non-glacial component for OIS stage 2 and 3 because they were deposited after the cessation of glacial flour input (see Figure 2 in Reynolds et al. 2004 – this issue) following the last glacial maximum, and before marshes formed around the mouths of streams and removed most of the fluvial sediment input to the lake (Bradbury et al. 2004 – this issue). For these samples, MS and ARM are

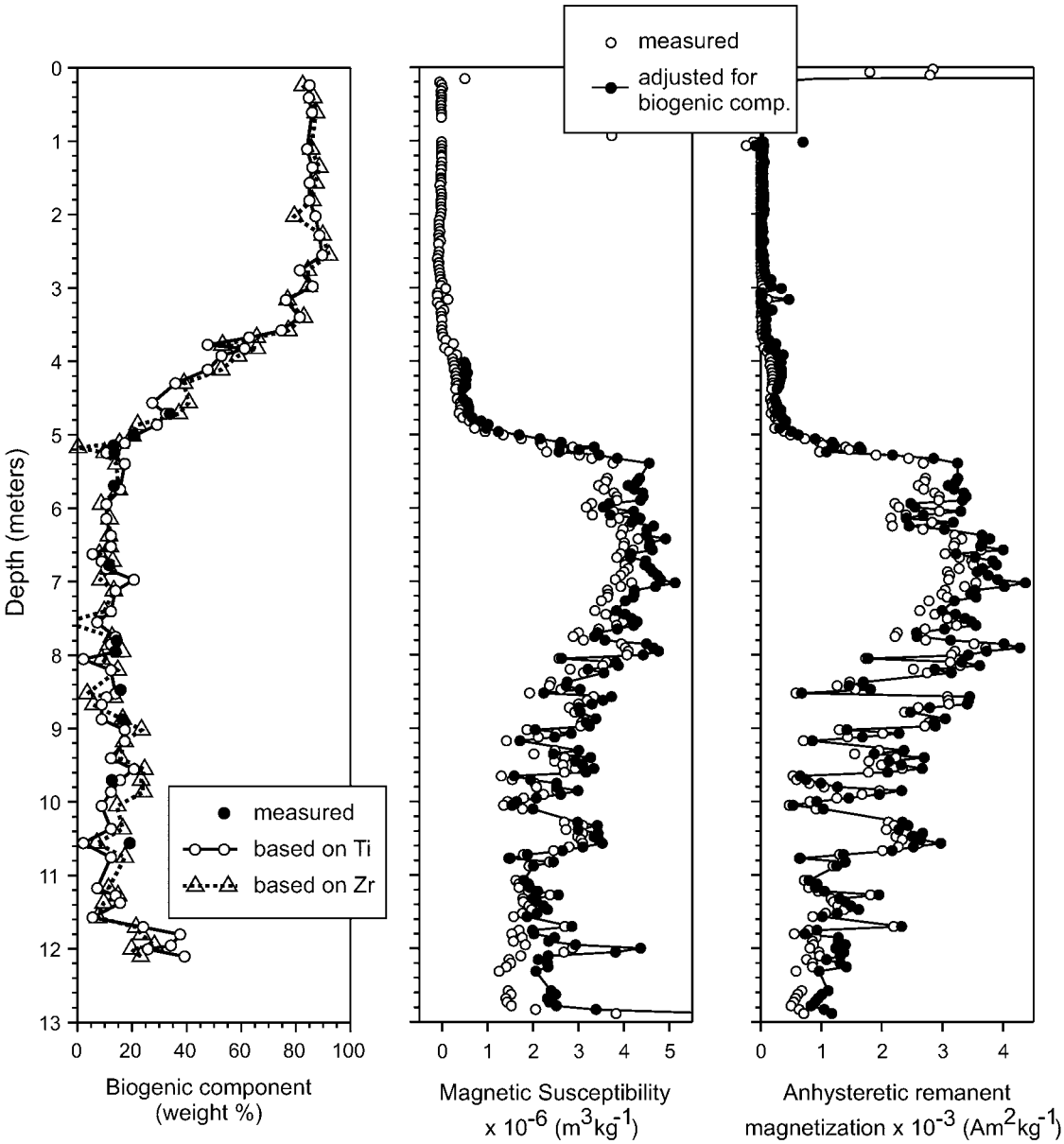

Figure 2. Biogenic component, magnetic susceptibility (MS), and anhysteretic remanent magnetization (ARM) of the Caledonia Marsh core. Using the samples for which biogenic silica was measured for calibration, the biogenic component (BC) was computed as $BC = (1-Ti/0.593) \times 100$ and as $BC = (1-Zr/177) \times 100$ where the Ti and Zr concentrations are in % and ppm, respectively. Magnetic property measurements were adjusted to a biogenic component-free basis using the Ti-based values. It was assumed that MS and ARM of the biogenic component are zero. In fact, MS of the biogenic component is very small and negative. Therefore, the correction was not applied to MS values for samples above 4 m because these samples have such low MS that the diamagnetism of the biogenic component is significant.

uniformly low. The samples contain largely fine to coarse silt and their grain-size distributions, which are highly similar, peak at about 30 μm.

An average grain-size distribution was determined for 13 samples in the interval 6.37–7.65 m. These samples, which contain both glacial flour and non-glacial sediments, were chosen because they represent a contiguous section of core having uniformly high content of glacial flour based on magnetic properties (Figure 2 and Table 1). These samples

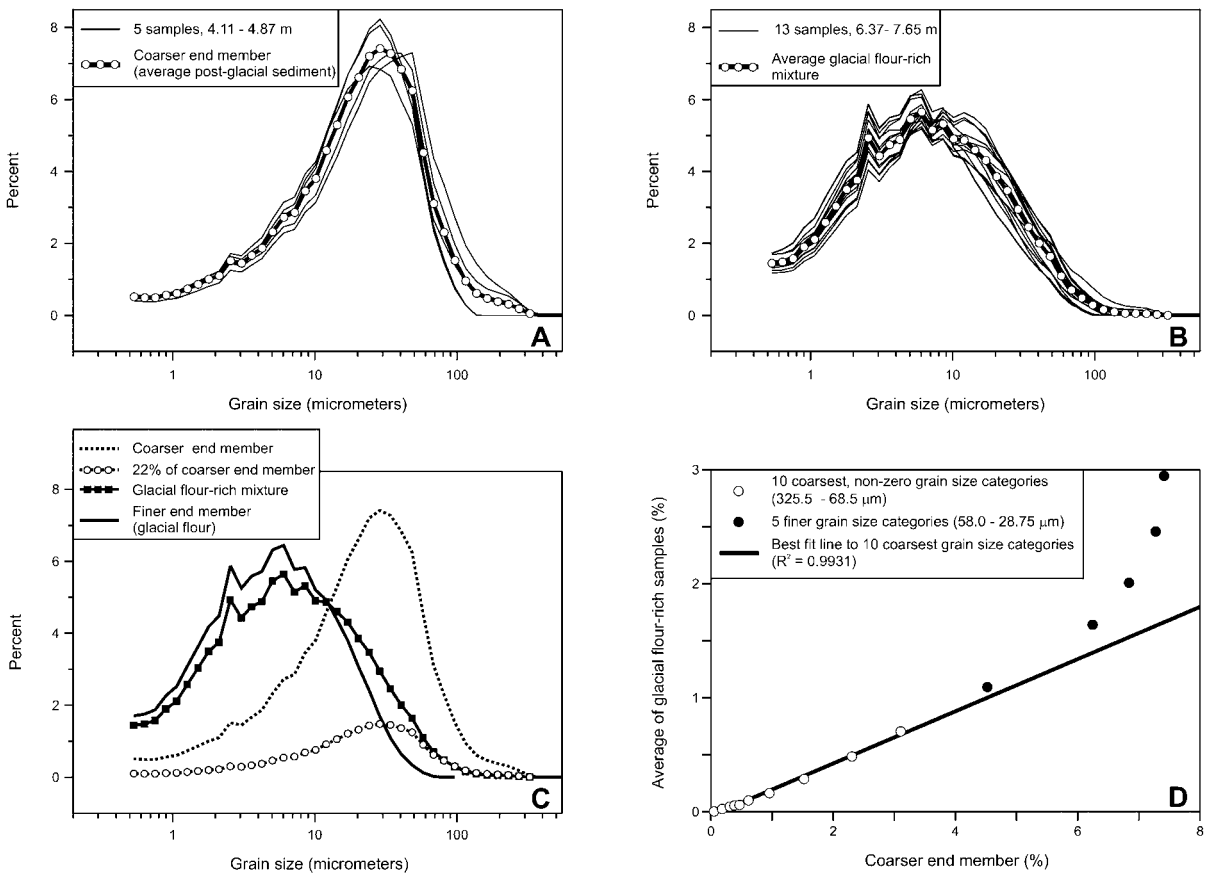

Figure 3. Calculation of the grain-size distributions of the coarser and finer end members. (A) Distributions for five post-glacial samples and the coarser end member. (B) Distributions for 13 glacial flour-rich samples and their average. (C) Grain-size distributions for the coarser end member and average glacial flour-rich samples (from A and B), and the computed distribution for the finer end member. (D) Plot of the grain size distribution for the coarser end member *versus* the average distribution for glacial flour-rich samples. The 15 coarsest (nonzero) grain size categories are shown.

comprise mostly fine silt and clay (Figure 3B). Their grain size distributions peak at about 6 μm and contrast markedly with that of the non-glacial end-member, which peaks at about 30 μm.

Although the grain-size distributions of the non-glacial end-member and glacial flour-rich sediments differ greatly, the coarse tails of the distributions are closely similar (Figure 3C). This is interpreted to indicate that the coarser particles in the glacial sediments are derived solely from non-glacial material. This relation is examined more quantitatively by plotting the coarse end of grain-size distribution of the average glacial sediment *versus* that of the non-glacial end-member (Figure 3D). The 10 coarsest grain-size categories, spanning 68.5–325.5 μm, define a strong linear relation. For smaller grain-size categories, the shapes of the grain-size distributions diverge. For the nine and 10 coarsest grain-size categories, the slopes of the best-fit lines are 0.21 and 0.23, respectively, indicating that on average the non-glacial component of the 13 glacial sediment samples is about 22%.

Using this result, the grain-size distribution and magnetic properties of glacial flour are easily calculated. For each grain-size category, subtracting 22% of the non-glacial value from the average glacial-sediment value and renormalizing the resultant distribution to 100% yields the glacial flour grain size distribution (Figure 3C). Similar calculations yield magnetic properties for glacial flour (Table 1).

Table 1. Average magnetic properties of lithic material.

	N	Magnetic susceptibility ($m^3\ kg^{-1}$)	Anhysteretic remanent magnetization ($Am^2\ kg^{-1}$)	Comment
Less magnetic (weathered, non-glacial) component	5	6.23×10^{-7} (2.21×10^{-7})	2.96×10^{-4} (7.13×10^{-5})	4.11–4.87 m
Highly magnetic (glacial flour-rich) samples	13	4.37×10^{-6} (4.47×10^{-7})	3.58×10^{-3} (4.37×10^{-4})	6.37–7.65 m
More magnetic (glacial flour) component		5.43×10^{-6}	4.51×10^{-3}	Calculation based on interpretation of sediment grain-size data that highly magnetic samples contain 78% glacial flour.
Ratio (more magnetic:less magnetic)		8.72	15.2	Fine-grained titanomagnetite was destroyed by weathering.

Note: Standard deviations are shown in parentheses.

Non-glacial and glacial flour components

For each sample, the contents of the lithic end-members can be computed using magnetic properties (model 1) and grain size-data (model 2).

For model 1, the percentage of glacial flour in a sample (GF_{SAMP}) was computed as:

$$GF_{SAMP} = (100 - B)(M_{SAMP} - M_{NG})/(M_{GF} - M_{NG}),$$

where B is the percentage of biogenic component; M is the magnitude of a magnetic property (i.e., MS or ARM); the subscript, SAMP, indicates sample values adjusted for the biogenic component; and the subscripts, NG and GF, refer to the values for the non-glacial and glacial flour end-members, respectively (Table 1). The estimates of glacial flour based on MS and ARM are similar (Figure 4) and display the same variations evident in the magnetic property data (Reynolds et al. 2004 – this issue). Content of glacial flour is relatively low, mostly 15–40%, from the base of the core to a depth of about 10.8 m. Starting at about 10 m there is a general increase in glacial flour with contents reaching about 80% at 7 m. Contents remain generally high to 5.4 m and then decrease abruptly to insignificant levels by 5 m. Superimposed on this general pattern are well-defined higher frequency variations. In the lower part of the core, glacial flour content based on ARM data tends to be lower than content based on MS data. This disparity increases downward. Between 8 m and 10.8 m local minima defined by ARM tend to be significantly lower than those defined by MS, whereas the local maxima are nearly coincident. Below 10.8 m nearly all ARM-based values are significantly less than the corresponding MS values.

For model 2, the percentage of glacial flour in a sample was determined by comparing the observed grain-size distribution to computed distributions for mixtures of the two end-members. For each sample, linear fits were computed between the sample data and each of 101 mixtures, ranging in glacial flour content from 0 to 100% at 1% increments. The glacial flour content was taken as equal to that of the mixture that yielded the highest correlation coefficient, R^2. Most sample distributions could be closely approximated by combinations of the end-members (Figure 5A and B) as indicated by maximum values of R^2 that exceeded 0.87 for all but four samples. Three of these samples are at the bottom of the core and contain a high proportion of material coarser than the non-glacial component of the model (see sample 12.83 m, Figure 5A). This coarse material is probably reworked ash from the underlying Mt. Saint Helens C tephra (Reynolds et al. 2004 – this issue). The fourth sample, at 7.95 m (not shown in Figure 5A), also contains a coarse component not accounted for by the model. These four samples were eliminated from further analysis. For the remaining samples, small discrepancies between observed and

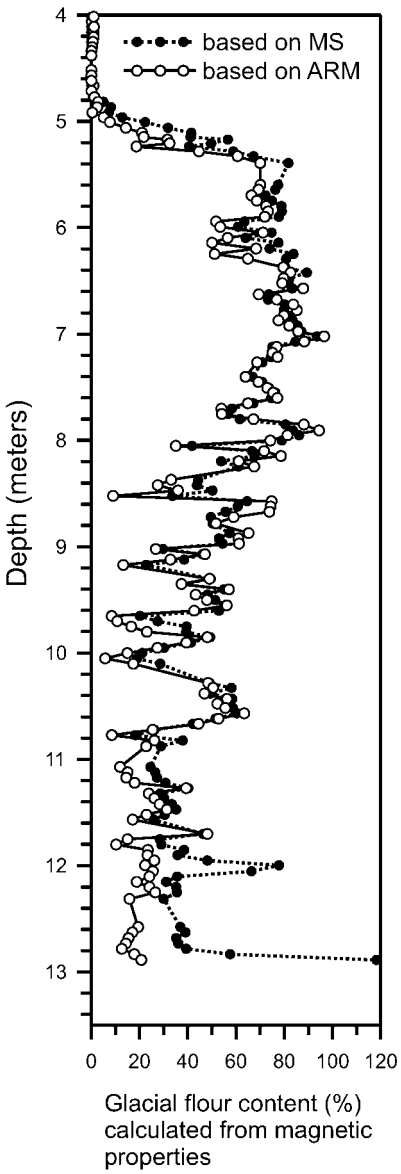

Figure 4. Glacial flour content calculated from magnetic susceptibility and from anhysteretic remanent magnetization.

best-fit grain-size distributions also appear to be mostly the result of more relatively coarse material than can be produced by combining the end-members. Therefore, for lower values of R^2 (e.g., samples 9.75, 8.52 and 6.25 m) model 2 may tend to underestimate the glacial flour content.

The two models produce similar patterns of variations in calculated glacial flour content (Figure 5C). Most of the short wavelength variations, as well as the long-term trends that are present in model 1 are also present in model 2. Above about 8 m, the two models yield nearly identical values. Below this depth, however, model 2 generally indicates somewhat higher glacial flour contents than model 1, even though, as noted above, there is an apparent tendency for model 2 to underestimate glacial flour.

A geologically reasonable explanation for the lower values produced by model 1 is that magnetic properties of glacial flour are not constant, as was assumed. Glacial flour will incorporate weathered material from soils and older drift as well as fresh volcanic fragments. The proportion of less magnetic weathered material is likely to be higher prior to the glacial maximum because, at their maximum extent, the glaciers will have removed much of the weathered material and will be generating the greatest amounts of fresh material. This explanation also accounts for the lower glacial flour contents calculated using ARM, rather than MS, in model 1, because the strong grain-size dependence of ARM makes ARM more sensitive to weathering than MS (Table 1). The model 2 results, therefore, probably give a somewhat more accurate estimate of glacial flour content prior to the last glacial maximum. Model 1, however, gives better temporal resolution because it incorporates more data.

Revised age–depth relations

Models comprising straight-line segments that connect points on an age–depth plot often have abrupt changes in slope where line segments intersect. The locations and magnitudes of these changes are strongly affected by the choice of samples for dating. A major goal in refining the age–depth relations was to minimize these abrupt changes in slope that are artifacts of the interpolation procedure. Such changes in slope produce large spurious changes in calculated flux. The revised age model (Figure 6) was based on the mass accumulation of the non-glacial lithic material, because the flux of this component is likely to be less variable than the flux of glacial flour.

The properties of each 1.5-cm thick sample (i.e., density and content of the three components) are assumed to be representative of the core interval

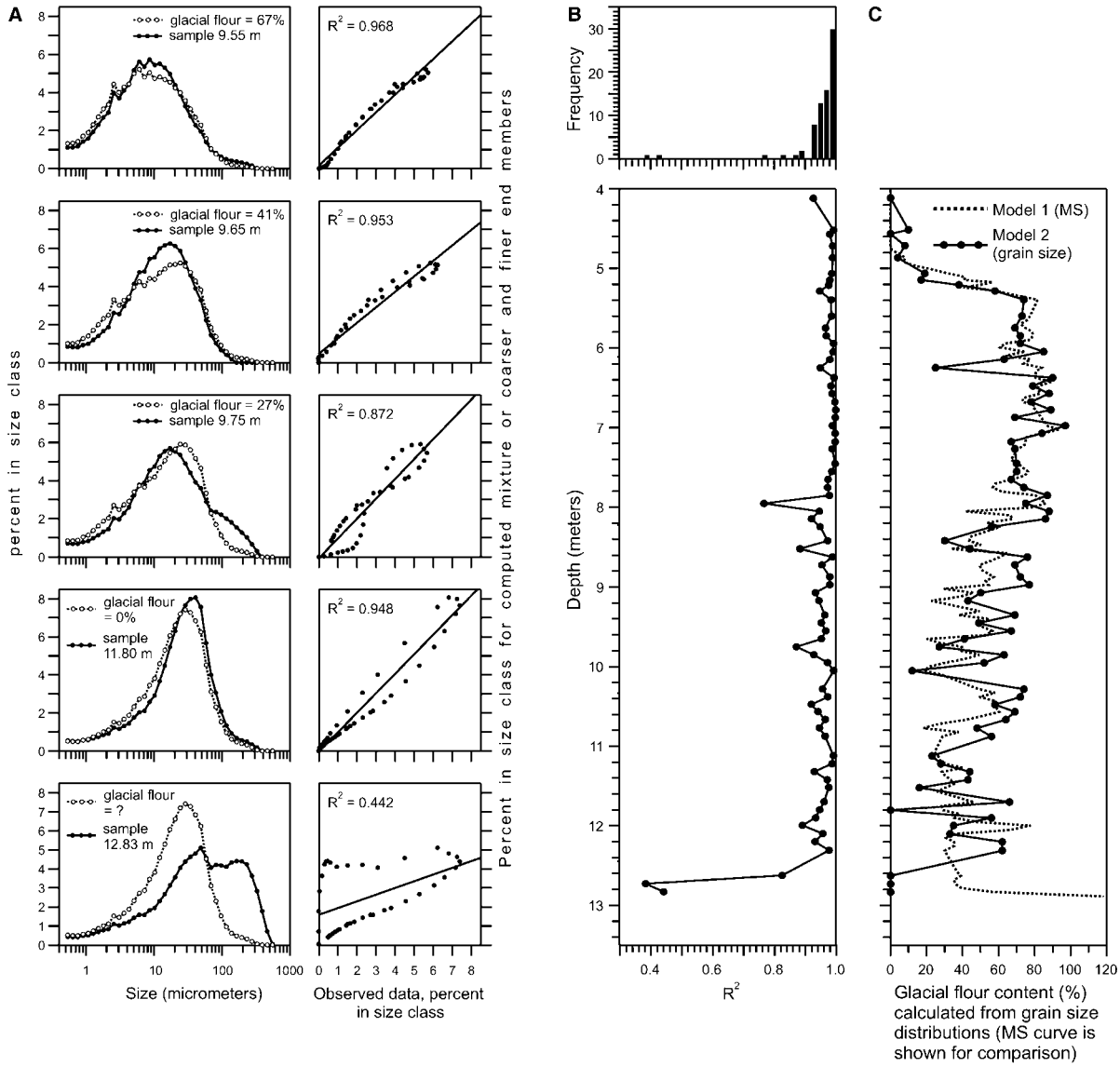

Figure 5. Determination of glacial flour content from grain size data. (A) Comparison of observed grain size distributions for selected samples and calculated distributions for the 'best-fit' mixtures of the coarser and finer end members. (B) Maximum values of the correlation coefficient, R^2, determined by comparing grain size distribution of individual samples to those calculated for mixtures of the end members. Mixtures were calculated at 1% increments. (C) Content of glacial flour calculated from grain size data.

extending half way to the underlying and overlying samples (typically about 5 cm). An incremental mass of non-glacial material was calculated for each of these core intervals. At a given depth, the cumulative mass is the sum of all of the overlying incremental masses.

Fifth order polynomials were fit to the cumulative masses of the non-glacial lithic fractions (from models 1 and 2) and the calibrated ^{14}C age data provided by Colman et al. (2004 – this issue) to produce refined age-depth relations. These curves fit the observed data closely and have gentle changes in slope (Figure 6). The curves indicate a nearly constant rate of accumulation of the non-glacial fraction between 33 and 15 ka and then smoothly decreasing accumulation into the

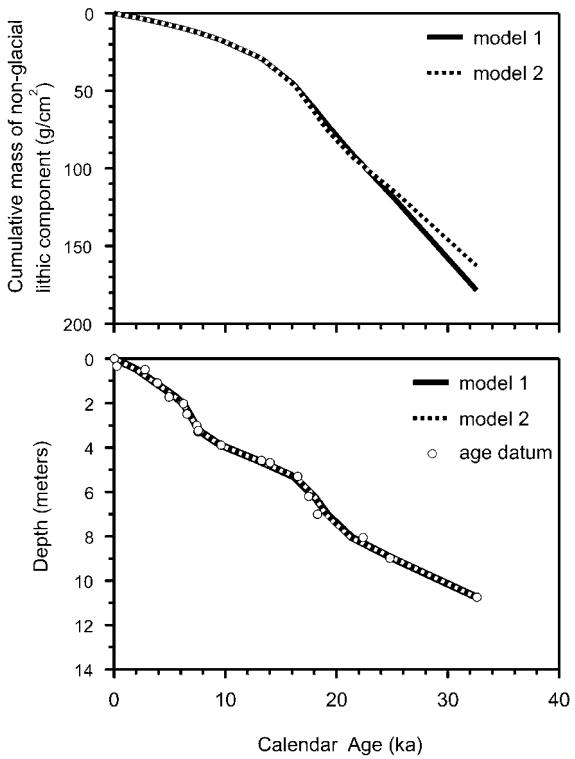

Figure 6. Revised age models for data presented by Colman et al. (2004 – this issue). Fifth-degree polynomials, constrained to pass through the origin, were fit to the ages and cumulative mass of non-glacial lithic component and then transferred to a depth *versus* age plot.

Holocene. For the older part of the section, the mass accumulation curves diverge; model 2 results indicate a slower accumulation of non-glacial material. This difference is the direct result of the generally lower content of glacial flour computed for model 1 in this part of the core as described previously. There is no significant difference, however, in the depth–age curves for the two models. The polynomials were used to adjust ages for each of the dated horizons. For reasons explained below, however, individual sample ages calculated from the polynomials were not used in the final flux calculations. Instead, the final age–depth functions are compromises, consisting of linear segments with sample ages interpolated on the basis of depth between the *adjusted* ages. These functions have slightly more abrupt changes in slope than do the polynomials but less abrupt changes than are produced by linear interpolation between *measured* ages.

Calculation of flux

The flux of glacial flour was determined independently for models 1 and 2. For each sample, the flux was calculated as the quotient of the incremental mass of glacial flour and incremental age corresponding to the same intervals used to calculate the incremental masses of non-glacial lithic material for the refined chronology.

Errors in flux are highly dependent on the method used to calculate incremental ages. When age increments are determined using the polynomials, glacial flour-rich portions of the section yield flux curves containing high amplitude, short wavelength variations (Figure 7A). These high-frequency variations are probably noise because the patterns of variation differ for models 1 and 2. The source of this noise can be readily understood by noting that, in this method, age increments are proportional to the content of non-glacial lithic material. Therefore, flux is proportional to GF/(1−GF), where GF is the fraction of glacial flour. For high percentages of glacial flour, relatively small errors in the estimate of content produce large errors in computed flux (Figure 7B). To avoid these errors, incremental ages were linearly interpolated on the basis of depth between adjusted ages for each of the dated horizons. This method produces age increments that are independent of the glacial flour content, and it produces similar results for both models.

Glacial history

Flux of glacial flour from cored Upper Klamath Lake sediments constitutes a continuous record of glacial history spanning the late Wisconsin. The record integrates input from a number of alpine glaciers on the eastern flank of the southern Cascade Range west and northwest of Upper Klamath Lake. These glaciers include those in drainages arising on high topography east of the Cascade crest in the area of the Mountain Lake Wilderness (Figure 8) and on the northeast flank of Pelican Butte, as well as several glaciers that descended from the Cascade crest northwest of the lake (see Figure 1 of Reynolds et al. 2004 – this issue).

Carver (1973) described the areal distribution and stratigraphic relations of glacial deposits in the

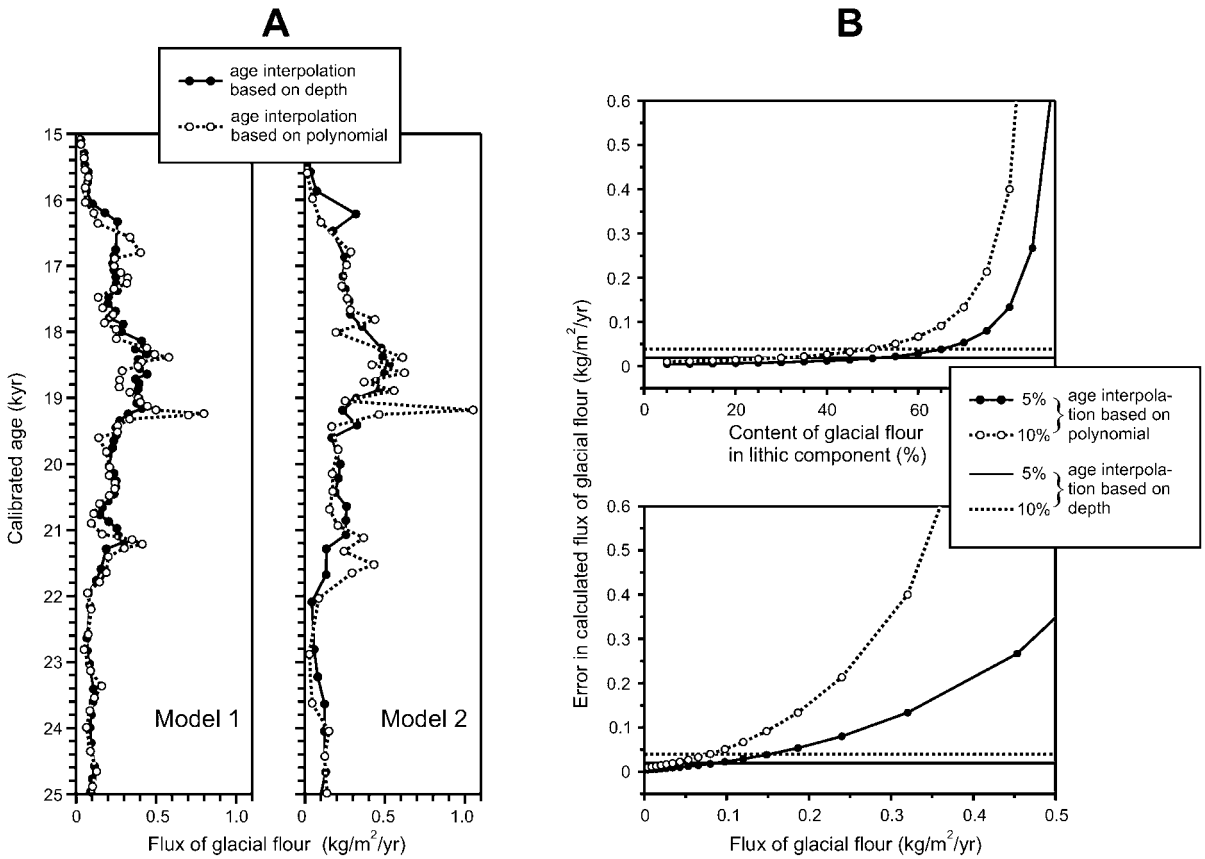

Figure 7. Comparison of the effect of choice of method for age interpolation on calculated flux. (A) Flux *versus* age for a portion of the record from the Caledonia Marsh core. (B) Theoretical errors in flux. Errors are calculated for 5 and 10% over estimates of glacial flour content. For the calculation, the slopes of the polynomial and depth *versus* age curve were 8 gm/ky and 55.5 cm/ky, respectively. These slopes are the approximate values for 18 ka (Figure 6).

Mountain Lakes Wilderness Area (Figure 8) and along the crest of the Cascade Range to the west of Upper Klamath Lake. He did not acquire any absolute dates, but used morphological characteristics and weathering criteria to distinguish deposits of several ages including two late Wisconsin units. He named the older more extensive unit the Waban drift, and the younger unit, which is restricted to high elevations, the Zephyr Lake drift. These units probably correlate, respectively, with the Suttle Lake and Canyon Creek members in the Metrolius River area in northern Oregon (Scott 1977), the Evans Creek and McNeeley drifts in the area of Mt. Rainier (Crandall and Miller 1974; Porter et al. 1983), and the preHyak members and Hyak Member of the Lakedale Drift in the southern Northern Cascades (Porter 1976).

Carver (1973) subdivided the Waban drift into several parts representing different stages in the growth and recession of Waban glaciers. The oldest subunit, the *South Pass moraine deposits*, include a large terminal moraine and a set of nested recessional moraines that were interpreted to represent an early glacial advance and recession. This unit was over ridden and truncated by subsequent advance of ice to the maximum extent of Waban glaciers. The *outer moraine deposits* comprise relatively small terminal moraines and numerous small closely spaced recessional moraines. The small size and great number of these moraines was interpreted to indicate a short maximum stand followed by a period of slow retreat. Rapid glacial retreat followed with widespread formation of *stagnant ice deposits*, which are characterized by numerous

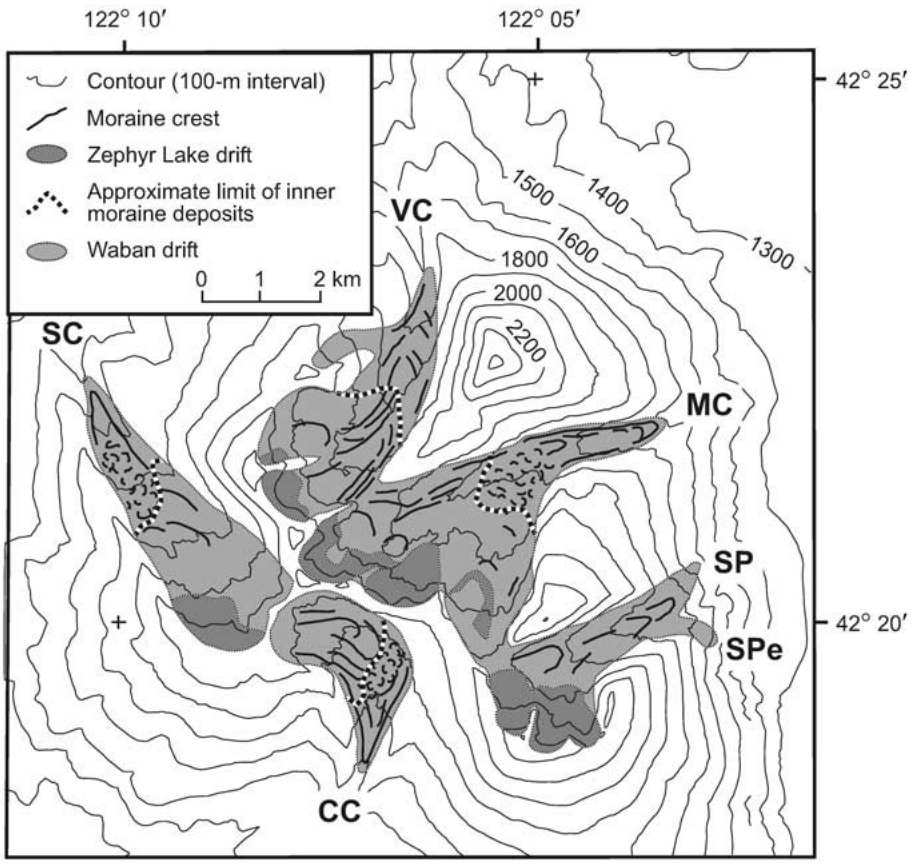

Figure 8. Map of Waban and Zephyr Lake drifts in the Mountain Lakes Wilderness area, southern Oregon; modified from Figure 6 of Carver (1973). The Seldom Creek (SC), Varney Creek (VC), Moss Creek (MC), and South Pass (SP) glaciers drained into Upper Klamath Lake but the Clover Creek (CC) glacier did not. South Pass moraine deposits (Spe) are from an early phase of the Waban period. The location of the Mountain Lakes Wilderness area is shown in Figure 1 of Reynolds et al. (2004 – this issue).

kettles in chaotic ground moraine. Up valley from the stagnant ice deposits are small nested moraines. These *inner moraine deposits* indicate a period of relative stability and slow back wasting following the rapid glacial retreat. Carver (1973) indicated that the Zephyr Lake drift could have been formed either during a late phase of the Waban period or somewhat later in a separate glacial period.

Because glacial sediments may at times be sequestered and at other times flushed from storage, the precise timing of glacial flour discharge with respect to changes in glacial extent cannot generally be determined with certainty. Leonard (1997) concluded that glacial flour in sediments from a Canadian lake closely reflect the extent of alpine glaciation when averaged over a few tens of years. This conclusion is probably valid for Upper Klamath Lake sediments as well. The glaciers that contributed sediment to Upper Klamath Lake filled relatively steep valleys with little area for storage (Figure 8). The valleys contain numerous lakes, but these are all small kettles and tarns that were ice filled during the Waban glaciation. The tarns would have trapped glacial sediments, however, when only small cirque glaciers were present and the tarns were devoid of ice. In addition, integration of sediment from a number of glaciers would tend to smooth the effects of short-term sediment storage/discharge events that affected individual glaciers. For model 1, samples represent time intervals ranging from about 260 years (prior to 22 ka) to about 120 years (from 22 to 15 ka). Consequently, a single short-lived event, such as

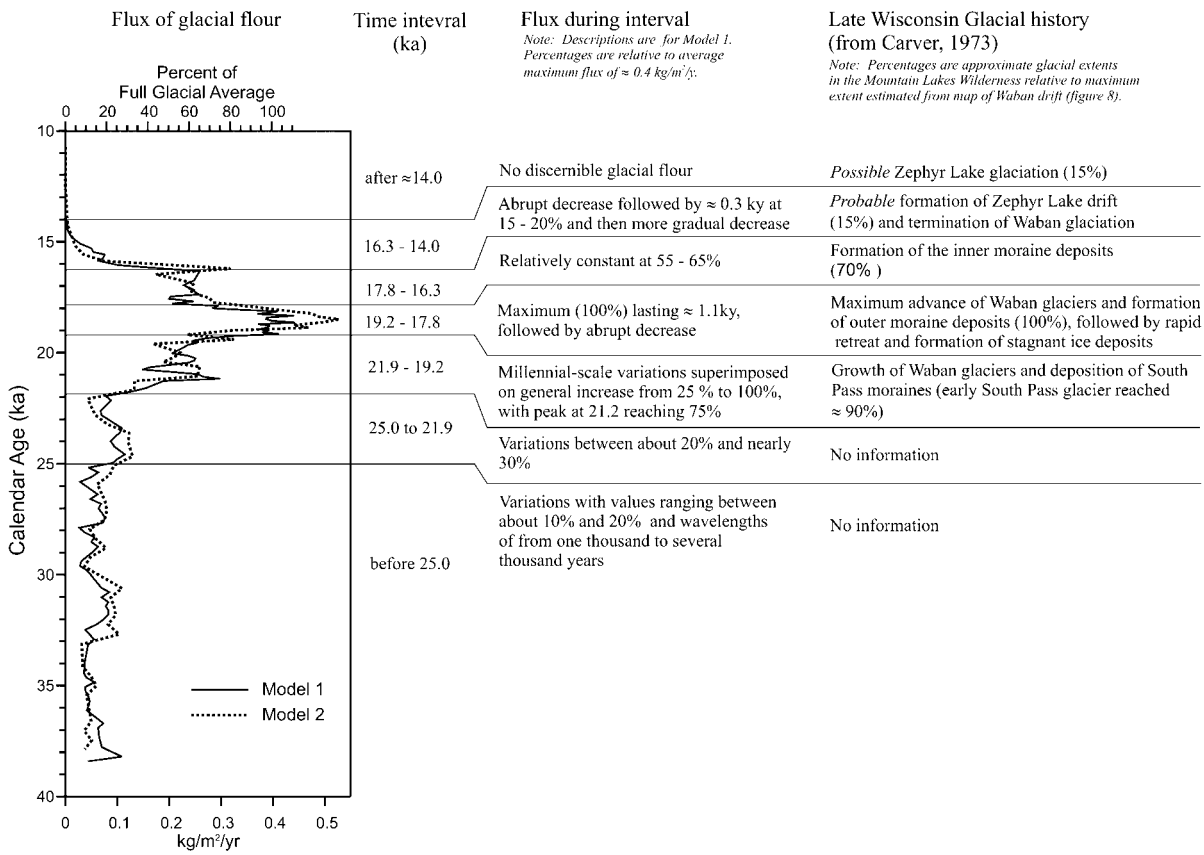

Figure 9. Flux of glacial flour from Upper Klamath Lake with proposed correlation to glacial history interpreted from glacial deposits.

flushing of glacial flour, will probably not affect more than one or two samples. Such short-lived events may contribute to some of the shortest wavelength features in the record, such as the spikiness during the period of maximum flux between 18 and 19 ka (Figure 9). The longer wavelength variations in flux, however, probably are closely related to glacial advances and retreats.

The calibrated ^{14}C-dated record of glacial flour provides a chronology for late Wisconsin glacial history in the area (Figure 9). Clearly, the Waban glacial period began about 22 ka and ended at 14 ka. At 21.9 ka, after a period of over 15 000 years during which glaciers of limited extent waxed and waned with wavelengths ranging from roughly one thousand to several thousand years, glaciers began to expand reaching their maximum extent between 19.2 and 18.1 ka. Glaciers began to retreat at 18.1 ka and disappeared by 14 ka. Details of the glacial flour record tentatively can be correlated with the subunits of the Waban drift (Figure 9). The advance that formed the *South Pass moraine deposits* occurred during the period of general increase in glacial flour between 21.9 and 19.2 ka, possibly coinciding with the peak at about 21.2 ka. Formation of the *outer moraine deposits* occurred during the peak output of glacial flour between about 19.2 and 18.1 ka. Rapid glacial retreat and formation of *stagnant ice deposits* coincided with the abrupt decrease in glacial flour beginning at about 18.1 ka. Glaciers then stabilized and formed the *inner moraine deposits* over about 1500 years, while the flux of glacial flour remained nearly constant. The flux then declined again, first abruptly and then more gradually, reaching undetectable levels by 14.0 ka. These intervals of rapid and more gradual decrease are separated by a period of several hundred years during which the flux again remained nearly constant. The Zephyr Lake drift probably formed during this final period of

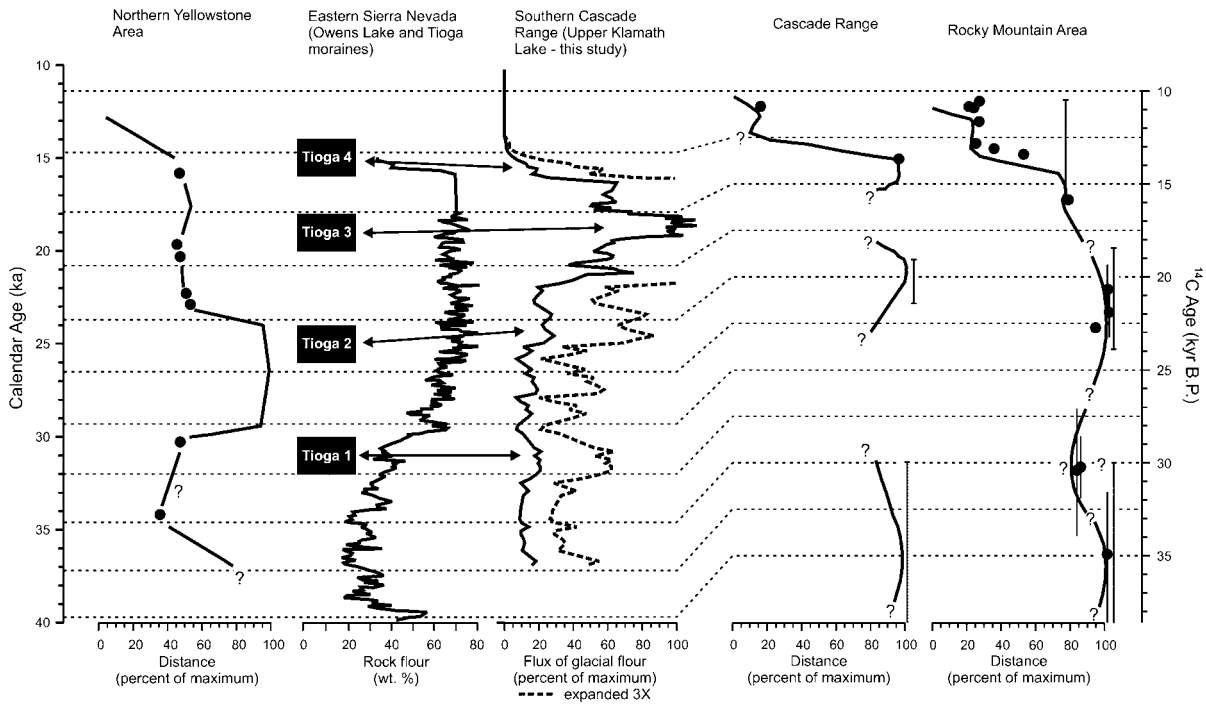

Figure 10. Comparison of the glacial flour record from Upper Klamath Lake to regional reconstructions of alpine glaciations. For the eastern Sierra Nevada; (1) rock flower content in Owens Lake sediments was computed from chemical analyses of the clay-sized fraction (curve modified from Figure 9 of Bischoff and Cummins 2001), and (2) ^{36}Cl ages were determined for four ages of late Wisconsin (Tioga) moraines (Phillips et al. 1996). (Note: The boxes centered on ages of Tioga moraines are 2 kyr wide; arrows indicate possible correlative features in the Upper Klamath Lake record.) The other regional reconstructions (with age control shown by points and error bars) are modified from Figure 2 of Clark and Bartlein (1995).

relative stability and subsequent slow retreat. If the Zephyr Lake drift formed at a later time, then sediment from the Zephyr Lake glaciers must have been trapped in tarns and did not reach Upper Klamath Lake. The proposed correlation suggests a strong, nearly linear, relation between glacial extent and flux of glacial flour (Figure 9).

Comparison to other glacial records

Comparing the Upper Klamath Lake record to other records of glacial history reveals both similarities and differences in timing and amplitude. The Last Glacial Maximum (LGM) occurred at about 21 ka (Imbrie et al. 1984), significantly before late Wisconsin glaciers in the southern Cascades reached their maximum extents (Figure 9). During the LGM, global ice volumes were at maximum levels from about 22 to 19 ka, and then declined sharply at about 19 ka (Yokoyama et al. 2000). Growth of Waban glaciers corresponds closely to the period of maximum global ice volume. Waban glaciers maintained their maximum extents until about 18 ka, about 1000 years after global ice volume declined sharply.

Maximum glaciations of the southern Cascades and the eastern Sierra Nevada, as indicated by the rock flour record from Owens Lake (Bischoff and Cummins 2001), overlap in time (Figure 10), although the Owens Lake record indicates earlier growth of ice. The records indicate that deglaciations in the two regions nearly coincided. The apparent differences between these records may be due in part to the use of rock flour content, rather than flux, for the Owens Lake record. Tioga moraines in the area of Owens Lake fall into four age ranges; 31, 25, 19 and 16 ka (Phillips et al. 1996). Taken at face value, there is a strong correspondence between the timing of Tioga glacial

advances and four of the most prominent maxima in the Upper Klamath Lake record (Figure 10), although the precision of dating precludes unequivocal correlation. The Tioga 2 was the largest, and the Tioga 3 was the second largest of the four advances. In the southern Cascades, however, the advance that corresponds to Tioga 3 was much more extensive than the advance that apparently correlates with Tioga 2.

The timing of the last major glacial retreat in the southern Cascades, beginning at about 16 ka, is similar to that in more northern parts of the Cascade Range, the Yellowstone area, as well as other parts of the Rocky Mountains (Figure 10). Records from these other areas suggest that glacial extents during much of OIS 3 were comparable to those of OIS 2. In contrast, in comparison to the maximum Waban extent, southern Cascade glaciers during this period were quite small. In large part, this difference may be due to the relatively low elevation of the Cascades (peaks mostly <2500 m) in the area of Upper Klamath Lake. Because of the low elevations, snow line would have to be much lower before any glaciers could exist in the area. Under current conditions, the regional snowline is probably about 2900 m. Throughout OIS 3, equilibrium line altitudes must have been no higher than during the Zephyr Lake period, 2200–2300 m (Carver 1973).

Summary

(1) Magnetic properties and bulk sediment grain size provide means of calculating the content of glacial flour in Upper Klamath Lake sediments. The success of these methods depends on the lack of significant post-depositional alteration affecting bulk sediment grain size or magnetic properties.

(2) In Upper Klamath Lake sediments, flux of glacial flour appears to largely reflect glacial extent. If the glacial history of the Mountain Lake Wilderness (Figure 8) is representative of the entire area that contributed glacial flour to Upper Klamath Lake, and the correlations presented in Figure 9 are correct, then the relation between areal extent and flux is nearly linear.

(3) Alpine glacial deposits have been studied throughout much of the Cascade Range, yet few ages can be assigned to these deposits with confidence (Porter et al. 1983; Clark and Bartlein 1995). The Upper Klamath Lake record contains information about timing and duration of glacial advance, still stand, and recession, and provides an essentially continuous, high-resolution, ^{14}C-dated record of late Wisconsin glaciation in the southern Cascade Range.

(4) During OIS 3, glaciers in the Upper Klamath Lake catchment were of limited extent in comparison to the extents indicated by regional records from other areas of the western United States. These small, southern Cascade glaciers fluctuated in size with periods of from one to several thousand years. Glacial extents during OIS 3 were similar to the Zephyr Lake period (Figure 8), if the Zephyr Lake drift formed at about 15.5 ka, near the end of the Waban glaciation (Figure 9). If the Zephyr Lake occurred later and ice-free tarns captured its glacial flour, then the earlier glaciers must have been of somewhat greater extent. Major expansion of late Wisconsin (Waban) glaciers began at ≈22 ka. Glaciers reached their maximum extent at about ≈19 ka, began to recede at ≈18 ka, and then stabilized for ≈1500 years. The final period of glacial recession began ≈16 ka (about the same time as late Wisconsin mountain glaciers began to decline throughout the western United States) and by 14 ka were no longer large enough to contribute measurable quantities of glacial flour to Upper Klamath Lake.

(5) Upper Klamath Lake lies in an active tectonic depression (Colman et al. 2000). Repeated down dropping has allowed accumulation of lake sediments that exceed 150 m in some localities (Liberty et al. 2000). Future coring of these sediments could provide a much longer glacial history for the southern Cascades, perhaps extending back through the penultimate glaciation.

Acknowledgements

This study benefited from discussions with K. Pierce and J. Yount. We are grateful for constructive reviews by P. Carrara, M. Kerwin, and J. Peck. This work was supported by the Earth Surface Dynamics Program of the US Geological Survey.

References

Benson L.V., Burdett J.W., Kashgarian M., Lund S.P., Phillips F.M. and Rye R.O. 1996. Climatic and hydrologic oscillations in the Owens Lake basin and the adjacent Sierra Nevada, California. Science 274: 746–749.

Bischoff J.L. and Cummins K. 2001. The Wisconsin glaciation of the Sierra Nevada (79 000–15 000 B.P.) as recorded by rock flour in sediments of Owens Lake, California. Quaternary Res. 55: 14–24.

Bischoff J.L., Fitts J.P. and Fitzpatrick J.A. 1997. Responses of sediment geochemistry to climate change in Owens Lake sediment: an 800 k.y. record of saline/fresh cycles in OL-92. In: Smith G.I. and Bischoff J.L. (eds), An 800,000-Year Paleoclimatic Record from Core OL-92, Owens Lake, Southeast California, Geological Society of America Special Paper 317, pp. 37–47.

Bradbury J.P., Colman S.M. and Dean W.E. 2004. Limnological and climatic environments at Upper Klamath Lake, Oregon during the past 45,000 years. J. Paleolim. 31: 167–188 (this issue).

Carver G.A. 1973. Glacial geology of the Mountain Lake Wilderness and adjacent parts of the Cascade Range, Oregon. PhD dissertation, University of Washington, Seattle, 76 pp.

Clark P.U. and Bartlein P.J. 1995. Correlation of late Pleistocene glaciation in the western United States with North Atlantic Heinrich events. Geology 23: 483–486.

Colman S.M., Bradbury J.P., McGeehin J.P., Holmes C.W., Edginton D. and Sarna-Wojcicki A.M. 2004. Chronology of sediment deposition in. Upper Klamath Lake, Oregon. J. Paleolim. 31: 139–149 (this issue).

Colman S.M., Rosenbaum J.G., Reynolds R.L. and Sarna-Wojcicki A.M. 2000. Post-Mazama (7Ka) faulting beneath Upper Klamath Lake, Oregon. Bull. Seismol. Soc. Am. 90: 243–247.

Crandall D.R. and Miller C.D. 1974. Quaternary stratigraphy and extent of glaciation in the Mount Rainier region, Washington. US Geological Survey Professional Paper 847.

Dunlop D. and Özdemir Ö. 1997. Rock Magnetism – Fundamentals and Frontiers. Cambridge University Press, New York, NY, 573 pp.

Hallet B., Hunter L. and Bogen J. 1996. Rates of erosion and sediment evacuation by glaciers: A review of field data and their implications. Global Planetary Change 12: 213–235.

Harbor J. and Warburton J. 1993. Relative rates of glacial and nonglacial erosion in alpine environments. Arctic Alpine Res. 25: 1–7.

Hicks D.M., McSaveney M.J. and Chinn T.J.H. 1990. Sedimentation in proglacial Ivory Lake, Southern Alps, New Zealand. Arctic Alpine Res. 22: 26–42.

Imbrie J., Hays J.D., Martinson D.G., McIntyre A., Mix A.C., Morley J.J., Pisias N.G., Prell W.L. and Shackleton N.J. 1984. The orbital theory of Pleistocene climate: support from a revised chronology of the marine ^{18}O record. In: Berger A., Imbrie J., Hays J., Kukla G. and Saltzman B. (eds), Milankovitch and Climate, Reidel, Dordrecht, pp. 269–305.

Karlén W. 1976. Lacustrine sediments and tree-limit variations as indicators of Holocene climatic fluctuations in Lappland, northern Sweden. Geografiska Ann. 58A: 1–34.

Karlén W. 1981. Laustrine sediment studies: A technique to obtain a continuous record of Holocene glacier variations. Geografiska Ann. 63A: 273–281.

Karlén W. and Matthews J.A. 1992. Reconstructing Holocene glacier variations from glacial lake sediments: Studies from Nordvestlandet and Jostedalsbreen-jotunheimen, southern Norway. Geografiska Ann. 74A: 327–348.

King J., Banerjee S.K., Marvin J. and Özedemir Ö. 1982. A comparison of different magnetic methods for determining the relative grain size of magnetite in natural materials: Some results from lake sediments. Earth Planetary Sci. Lett. 59: 404–419.

Leonard E.M. 1985. Glaciological and climatic controls on lake sedimentation, Canadian Rocky Mountains. Z. Gletscherkde Glazialgeol. 21: 35–42.

Leonard E.M. 1986. Use of sedimentary sequences as indicators of Holocene glacial history, Banff National Park, Alberta, Canada. Quaternary Res. 26: 218–231.

Leonard E.M. 1997. The relationship between glacial activity and sediment production: evidence from a 4450-year varve record of neoglacial sedimentation in Hector Lake, Alberta, Canada. J. Paleolimnol. 17: 319–330.

Liberty L.M., Pratt T.L., Madin I.P. and Lyle M. 2000. Late Quaternary sedimentation and slip rates for Upper Klamath Lake, Oregon: New measurements from high-resolution seismic reflection data. EOS 81: 1123–1124.

Liu X., Rolph T., Bloemendal J., Shaw J. and Liu T. 1995. Quantitative estimates of palaeoprecipitation at Xifeng, in the loess plateau of China. Palaegeogr. Palaeoclimatol. Palaeoecol. 113: 243–248.

Maher B.A., Thompson R. and Zhou L.P. 1994. Spatial and temporal reconstructions of changes in the Asian palaeomonsoon: A new mineral magnetic approach. Earth Planetary Sci. Lett. 125: 461–471.

Maher B.A., Zhou L.P. and Thompson R. 1994a. Reconstruction of palaeoprecipitation values for the Chinese loess plateau from proxy magnetic data. In: Funnell B.M. and Kay R.L.F. (eds), Palaeoclimate of the Last Glacial/Interglacial Cycle, Spec. Publ. NERC Earth Sci. Direct. 94/2, pp. 33–36.

Menking K.M. 1997. Climatic signals in clay mineralogy and grain-size variations in Owens Lake core OL-92, southeast California. In: Smith G.I. and Bischoff J.L. (eds), An 800,000-Year Paleoclimatic Record from Core OL-92, Owens Lake, Southeast California, Geological Society of America Special Paper 317, pp. 25–36.

Nesbitt H.W. and Young G.M. 1996. Petrogenesis of sediments in the absence of chemical weathering: effects of abrasion and sorting on bulk composition and mineralogy. Sedimentology 43: 341–358.

Phillips F.M., Zreda M.G., Benson L.V., Plummer M.A., Elmore D. and Sharma P. 1996. Chronology for fluctuations in late Pleistocene Sierra Nevada glaciers and lakes. Science 274: 749–751.

Porter S.C. 1976. Pleistocene glaciation in the southern part of the North Cascade Range, Washington, USA. Geol. Soc. Am. Bull. 87: 61–75.

Porter S.C., Pierce K.L. and Hamilton T.D. 1983. Late Wisconsin mountain glaciation in the western United States. In: Porter S.C. (ed.), Late Quaternary Environments of the United States, Vol. 1: University of Minnesota Press, The Late Pleistocene, Minneapolis, pp. 71–111.

Reynolds R.L. and King J.W. 1995. Magnetic records of climate change. Reviews of Geophysics; Supplement, US National Report to International Union of Geodesy and Geophysics 1991–1994, pp. 101–110.

Reynolds R.L., Rosenbaum J.G., Mazza N., Rivers W. and Luiszer F. 1998. Sediment magnetic data (83 to 18 m depth) and XRF geochemical data (83 to 32 m depth) from lacustrine sediment in core OL-92 from Owens Lake, California. US Geological Survey Open-file Report 98-132, 34 pp.

Reynolds R.L., Rosenbaum J.G., Rapp J., Kerwin M.W., Bradbury J.P., Colman S. and Adam D. 2004. Record of Late Pleistocene glaciation and deglaciation in the southern Cascade Range: I. Petrologic evidence from lacustrine sediment in Upper Klamath Lake, Oregon. J. Paleolim. 31: 217–233 (this issue).

Rosenbaum J.G. and Reynolds R.L. 2004. Basis for paleoenvironmental interpretation of magnetic properties of sediment from Upper Klamath Lake (Oregon): Effects of weathering and mineralogical sorting. J. Paleolim. 31: 253–265 (this issue).

Scott W.E. 1977. Quaternary glaciation and volcanism, Metolius River area, Oregon. Geol. Soc. Am. Bull. 88: 113–124.

Smith G.I. and Bischoff J.L. 1997. Core OL-92 from Owens Lake: Project rationale, geologic setting, drilling procedures, and summary. In: Smith G.I. and Bischoff J.L. (eds), An 800,000-Year Paleoclimatic Record from Core OL-92, Owens Lake, Southeast California. Geological Society of America Special Paper 317, pp. 1–8.

Smith G.I., Bischoff J.L. and Bradbury J.P. 1997. Synthesis of the paleoclimate record from Owens Lake core OL-92. In: Smith G.I. and Bischoff J.L. (eds), An 800,000-Year Paleoclimatic Record from Core OL-92, Owens Lake, Southeast California. Geological Society of America Special Paper 317, pp. 143–160.

Verosub K.L. and Roberts A.P. 1995. Environmental magnetism: Past, present and future. J. Geophys. Res. 100: 2175–2192.

Winchester J.A. and Floyd P.A. 1977. Geochemical discrimination of different magma series and their differentiation products using immobile elements. Chem. Geol. 20: 325–343.

Yokoyama Y., Lambeck K., De Deckker P., Johnston P. and Fifield L.K. 2000. Timing of the Last Glacial Maximum from observed sea-level minima. Nature 406: 713–716.